Lattice Boltzmann Simulation of Free-Surface Temperature Dispersion in Shallow Water Flows

Mohammed Seaïd[1],[*] and Guido Thömmes[2]

[1]*School of Engineering, University of Durham, South Road, Durham DH1 3LE, UK*

[2]*Fraunhofer-Institut für Techno-und Wirtschaftsmathematik, 67663 Kaiserslautern, Germany*

Abstract. We develop a lattice Boltzmann method for modeling free-surface temperature dispersion in the shallow water flows. The governing equations are derived from the incompressible Navier-Stokes equations with assumptions of shallow water flows including bed frictions, eddy viscosity, wind shear stresses and Coriolis forces. The thermal effects are incorporated in the momentum equation by using a Boussinesq approximation. The dispersion of free-surface temperature is modelled by an advection-diffusion equation. Two distribution functions are used in the lattice Boltzmann method to recover the flow and temperature variables using the same lattice structure. Neither upwind discretization procedures nor Riemann problem solvers are needed in discretizing the shallow water equations. In addition, the source terms are straightforwardly included in the model without relying on well-balanced techniques to treat flux gradients and source terms. We validate the model for a class of problems with known analytical solutions and we also present numerical results for sea-surface temperature distribution in the Strait of Gibraltar.

AMS subject classifications: 65M10, 78A48

Key words: Shallow water flows, free-surface temperature, lattice Boltzmann method, advection-diffusion equation, strait of Gibraltar.

1   Introduction

During the last years the increase of sea-surface temperature has attracted much interest in numerical methods for the prediction of its transport and dispersion. In many situations, this sea-surface temperature has detriment impact on the ecology and environment and may cause potential risk on the human health and local economy.

[*]Corresponding author.

URL: `http://www.dur.ac.uk/m.seaid`

Email: m.seaid@durham.ac.uk (M. Seaïd), thoemmes@mathematik.uni-kl.de (G. Thömmes)

Efficient and reliable estimates of impacts on the water quality due to free-surface temperature could play essential role in establishing control strategy for environmental protection. Introduction and utilization of such measures are impossible without knowledge of various processes such as formation of water flows and dispersion of sea-surface temperature. The mathematical models and computer softwares could be very helpful to understand the dynamics of both, water flow and sea-surface temperature dispersion. In this respect mathematical modeling of water flows and the processes of transport-dispersion of sea-surface temperature could play a major role in establishing scientifically justified and practically reasonable programs for long-term measures for a rational use of water resources, reduction of thermal discharge from particular sources, estimation of the impact in the environment of possible technological improvements, development of methods and monitoring facilities, prediction and quality management of the environment, etc. The success of the computational methods in solving practical problems depends on the convenience of the models and the quality of the software used for the simulation of real processes.

Clearly, the process of free-surface temperature dispersion is determined by the characteristics of the hydraulic flow and the temperature properties of the water. Thus, dynamics of the water and dynamics of the temperature must be studied using a mathematical model made of two different but dependent model variables: (i) a hydrodynamic variable defining the dynamics of the water flow, and (ii) a thermal variable defining the transport and dispersion of the temperature. In the current work, the hydrodynamic model is based on a two-dimensional shallow water equations while, a convection-diffusion equation is used for the free-surface temperature. For environmental flows, the shallow water system is a suitable model for adequately describing significant hydraulic processes. The different characteristics of thermal problems require an appropriate model to describe their dynamics, nevertheless for a wide class of thermal predictions the standard convection-diffusion equation can be used. The interaction between the two processes gives rise to a hyperbolic system of conservation laws with source terms.

Various numerical methods developed for general systems of hyperbolic conservation laws have been applied to the shallow water equations. For instance, most shock-capturing finite volume schemes for shallow water equations are based on approximate Riemann solvers which have been originally designed for hyperbolic systems without accounting for source terms such as bed frictions, eddy viscosity, wind shear stresses and Coriolis forces. Therefore, most of these schemes suffer from numerical instability and may produce nonphysical oscillations mainly because dicretizations of the flux and source terms are not well-balanced in their reconstruction. The well-established Roe's scheme [26] has been modified by Bermúdez and Vázquez [7] to treat source terms. This method has been improved by Vázquez [38] for general one-dimensional channel flows. However, for practical applications, this method may become computationally demanding due to its treatment of the source terms. Alcrudo and Garcia-Navarro [2] have presented a Godunov-type scheme for numerical solution of shallow water equations. Alcrudo and Benkhaldoun [1] have developed exact

solutions for the Riemann problem at the interface with a sudden variation in the to-pography. The main idea in their approach was to define the bottom level such that a sudden variation in the topography occurs at the interface of two cells. LeVeque [18] proposed a Riemann solver inside a cell for balancing the source terms and the flux gradients. However, the extension of this scheme for complex geometries is not trivial. Numerical methods based on surface gradient techniques have also been applied to shallow water equations by Zhou *et al.* [44]. The TVD-MacCormak scheme has been used by Ming-Heng [22] to solve water flows in variable bed topography. A different approach based on local hydrostatic reconstructions have been studied by Audusse *el al.* [4] for open channel flows with topography. The performance of discontinuous Galerkin methods has been examined by Xing and Shu [40] for some test examples on shallow water flows. A central-upwind scheme using the surface elevation instead of the water depth has been used by Kurganov and Levy [19]. Vukovic and Sopta [39] extended the ENO and WENO schemes to one-dimensional shallow water equations. Unfortunately, most ENO and WENO schemes that solves real flows correctly are still very computationally expensive.

In recent years, the Lattice Boltzmann (LB) method has been considered as an ef-ficient numerical tool for simulating fluid flows and transport phenomena based on kinetic equations and statistical physics. Because of its distinctive advantages over conventional numerical methods, the LB method has become an attractive algorithm for free-surface flows. Some numerical methods based on the gas kinetic theory have been proposed in [23,30,41] to study shallow water flows. Zhou [43] has studied an LB method for simulating shallow water flows. The LB method has also been successfully applied to shallow water equations which describe wind-driven ocean circulation by Salmon [27] and Zhong *et al.* [42]. Application of LB method to three-dimensional planetary geostrophic equations was performed by Salmon [28]. Feng *et al.* [13] stud-ied an LB method for atmospheric circulation of the northern hemisphere. It was concluded that the LB method is an efficient approach for simulation of shallow water flows. Implementation of the LB method for two-dimensional shallow equations in irregular domains and complex bathymetry was investigated by Thömmes *et al.* [34]. Recently, Banda *et al.* [5] has extended this method to pollutant transport by the shal-low water flows. It is noticed that all above LB methods have been mainly applied to the isothermal shallow water flows and no thermal sources have been accounted for. However, temperature can strongly interact with hydraulic in many situations of engineering interest and neglecting its effects may have significant consequences in the overall predictions. For a discussion on the thermal effects on hydraulic flows we refer to [10,21,24,29,37] and further references can be found therein. Therefore, our main objective in the present work is to extend the LB techniques to free-surface temperature dispersion in shallow water flows.

The purpose of this study is to develop an LB method for modelling free-surface temperature dispersion in the shallow water flows. The governing equations are de-rived from the incompressible Navier-Stokes equations with assumptions of shallow water flows including bed frictions, eddy viscosity, wind shear stresses and Corio-

lis forces. Assuming a low temperature differences, a Boussinesq approximation is used to incorporate the thermal effects in the momentum equation. The dispersion of free-surface temperature in shallow water flows is modelled by a convection-diffusion equation. In order to reconstruct macroscopic flow and temperature variables we consider two distribution functions in the LB method using the same lattice structure. The proposed method avoids upwind discretization procedures and Riemann problem solvers which are indisponsible in most conventional methods for the shallow water flows. Moreover, the bed frictions, wind shear stresses and Coriolis forces are straightforwardly included in the LB model without relying on well-balanced techniques to treat flux gradients and source terms. Several test examples including problems with analytical solutions are used to validate the LB method. As a final example we simulate a test example of sea-surface temperature dispersion in the Strait of Gibraltar. To the best of our knowledge, this is the first time that the LB method is used to simulate the free-surface temperature dispersion in the shallow water flows.

This paper is organized as follows: in section 2 we introduce the governing equations for depth-averaged models for sea-surface dispersion in shallow water flows. The lattice Boltzmann method is formulated in section 3. This section includes the LB method for shallow water equations and for the convection-diffusion equation. Section 4 is devoted for numerical results and applications. Concluding remarks are summarized in section 5.

2　Equations for free-surface flow and temperature distribution

Modelling free-surface temperature dispersion requires two sets of coupled partial differential equations. The first set of equations describes the water motion on the free-surface flow while, the second set of equations models the distribution of temperature on the water free-surface. In the present study, the flow is governed by the depth-averaged Navier-Stokes equations involving several assumptions including: (i) the domain is shallow enough to ignore the vertical effects, (ii) the pressure is hydrostatic, (iii) all the water properties are assumed to be constant with the expection of the temperature dependence of the density, which is accounted for using the Boussinesq approximation, and (iv) viscous dissipation of energy is ignored and any radiative heat losses are assumed to have occurred over a time scale small compared with that which characterizes the flow motion. Thus, the starting point for the derivation of the free-surface flow model is the three-dimensional incompressible Navier-Stokes/Boussinesq equations,

$$\frac{\partial u}{\partial x} + \frac{\partial v}{\partial y} + \frac{\partial w}{\partial z} = 0, \tag{2.1a}$$

$$\frac{\partial u}{\partial t} + u\frac{\partial u}{\partial x} + v\frac{\partial u}{\partial y} + w\frac{\partial u}{\partial z} + \frac{1}{\rho}\frac{\partial p}{\partial x} = \nu\Delta u + \frac{\partial}{\partial z}(\nu_V \frac{\partial u}{\partial z}) - \Omega v, \tag{2.1b}$$

$$\frac{\partial v}{\partial t} + u\frac{\partial v}{\partial x} + v\frac{\partial v}{\partial y} + w\frac{\partial v}{\partial z} + \frac{1}{\rho}\frac{\partial p}{\partial y} = \nu\Delta v + \frac{\partial}{\partial z}\left(\nu_V\frac{\partial v}{\partial z}\right) + \Omega u, \tag{2.1c}$$

$$\frac{\partial w}{\partial t} + u\frac{\partial w}{\partial x} + v\frac{\partial w}{\partial y} + w\frac{\partial w}{\partial z} + \frac{1}{\rho}\frac{\partial p}{\partial z} = \nu\Delta w + \frac{\partial}{\partial z}\left(\nu_V\frac{\partial w}{\partial z}\right) - g + F, \tag{2.1d}$$

where t is the time variable, $(x,y,z)^T$ the space coordinates, ρ the water density, $(u,v,w)^T$ the velocity field, p the pressure, Ω the Coriolis parameter, g the acceleration due to gravity, ν and ν_V are the coefficients of horizontal and vertical eddy viscosity, respectively. In (2.1),

$$\Delta = \frac{\partial^2}{\partial x^2} + \frac{\partial^2}{\partial y^2},$$

denotes the two-dimensional Laplace operator and the force term F is given according to the Boussinesq approximation as

$$F = g\alpha(T - T_\infty), \tag{2.2}$$

with α is the thermal expansion coefficient and T_∞ is the reference temperature. In the present work, we are interested in flows which occur on the water free-surface where assumptions of shallow water flows applied. In most shallow water modelling, the ratio of vertical length scale to horizontal length scale is very small. As a consequence, the horizontal eddy viscosity terms are typically orders of magnitude smaller than the vertical viscosity terms and their effect is normally small and obscured by numerical diffusion. Therefore most models either neglect these terms or simply use a constant horizontal eddy viscosity coefficient. In addition, assuming that the pressure is hydrostatic, the momentum equation in the vertical direction (2.1d) reduces to the following form

$$\frac{1}{\rho}\frac{\partial p}{\partial z} = -g + g\alpha\left(T - T_\infty\right). \tag{2.3}$$

Integrating vertically the continuity equation (2.1a) from the sea bed $z=-B$ to the sea surface $z=\eta$ and using the kinematic condition at the free surface leads to the free-surface equation

$$\frac{\partial \eta}{\partial t} + \frac{\partial}{\partial x}\left(\int_{-B}^{\eta} u\, dz\right) + \frac{\partial}{\partial y}\left(\int_{-B}^{\eta} v\, dz\right) = 0, \tag{2.4}$$

where $\eta(x,y,t)$ is the water surface elevation and $B(x,y)$ is the water depth measured from the undisturbed water surface. We also denote the total water depth by

$$h(x,y,t) = \eta(x,y,t) + B(x,y).$$

The boundary conditions at the water free-surface are specified by the prescribed wind stresses $\mathcal{T}_x^\omega$ and $\mathcal{T}_y^\omega$

$$\nu_V\frac{\partial u}{\partial z} = \mathcal{T}_x^\omega, \qquad \nu_V\frac{\partial v}{\partial z} = \mathcal{T}_y^\omega, \tag{2.5}$$

with the wind stresses $\mathcal{T}_x^\omega$ and $\mathcal{T}_y^\omega$ are given by a quadratic function of the wind velocity $(\omega_x, \omega_y)^T$ as

$$\mathcal{T}_x^\omega = C_\omega \omega_x \sqrt{\omega_x^2 + \omega_y^2}, \qquad \mathcal{T}_y^\omega = C_\omega \omega_y \sqrt{\omega_x^2 + \omega_y^2}, \tag{2.6}$$

where C_ω is the coefficient of wind friction. The boundary conditions at the bottom are given by expressing the bottom stress in terms of the velocity components taken from values of the layer adjacent to the sediment-water interface. The bottom stress can be related to the turbulent law of the wall, a drag coefficient associated with quadratic velocity or using a Manning-Chezy formula such as

$$-\nu_V \frac{\partial u}{\partial z} = \mathcal{T}_x^b, \qquad -\nu_V \frac{\partial v}{\partial z} = \mathcal{T}_y^b, \tag{2.7}$$

with $\mathcal{T}_x^b$ and $\mathcal{T}_y^b$ are the bed shear stresses defined by the depth-averaged velocities as

$$\mathcal{T}_x^b = \rho g \frac{u\sqrt{u^2 + v^2}}{C_z^2}, \qquad \mathcal{T}_y^b = \rho g \frac{v\sqrt{u^2 + v^2}}{C_z^2}, \tag{2.8}$$

where C_z is the Chezy friction coefficient. Thus, using the free surface equation (2.4) and the boundary conditions (2.6) and (2.7), and after standard approximations on convective terms, we obtain the two-dimensional vertically averaged shallow water equations rewritten in conservative form as

$$\frac{\partial h}{\partial t} + \frac{\partial (hU)}{\partial x} + \frac{\partial (hV)}{\partial y} = 0, \tag{2.9a}$$

$$\frac{\partial (hU)}{\partial t} + \frac{\partial}{\partial x}\left(hU^2 + \frac{1}{2}g'h^2\right) + \frac{\partial}{\partial y}(hUV)$$
$$= -g'h\frac{\partial B}{\partial x} - g\alpha h\frac{\partial (h\Theta)}{\partial x} + \nu\Delta(hU) + \frac{\mathcal{T}_x^\omega}{\rho} - \frac{\mathcal{T}_x^b}{\rho} - \Omega hV, \tag{2.9b}$$

$$\frac{\partial (hV)}{\partial t} + \frac{\partial}{\partial x}(hUV) + \frac{\partial}{\partial y}\left(hV^2 + \frac{1}{2}g'h^2\right)$$
$$= -g'h\frac{\partial B}{\partial y} - g\alpha h\frac{\partial (h\Theta)}{\partial y} + \nu\Delta(hV) + \frac{\mathcal{T}_y^\omega}{\rho} - \frac{\mathcal{T}_y^b}{\rho} + \Omega hU, \tag{2.9c}$$

where $g' = g(1 + \alpha T_\infty)$, Θ is the depth-averaged temperature, U and V are the depth-averaged horizontal velocities in x- and y-direction given by

$$\Theta = \frac{1}{h}\int_{-B}^{\eta} T\,dz, \qquad U = \frac{1}{h}\int_{-B}^{\eta} u\,dz, \qquad V = \frac{1}{h}\int_{-B}^{\eta} v\,dz.$$

The temperature distribution on the sea-surface can be correctly traced by a depth-averaged convection-diffusion equation of the form

$$\frac{\partial \Theta}{\partial t} + \frac{\partial}{\partial x}(hU\Theta) + \frac{\partial}{\partial y}(hV\Theta) = \lambda\Delta(h\Theta) + hQ, \tag{2.10}$$

where Q is the depth-averaged source term and λ is the depth-averaged diffusion coefficient. In practical situations the eddy viscosity ν and the eddy thermal diffusivity coefficients depend on water temperature, water salinity, water depth, flow velocity, bottom roughness and wind, compare [6, 16] for more discussions. For the purpose of the present work, the problem of the evaluation of eddy diffusion coefficients is not considered.

3   Lattice Boltzmann methods

The starting point for the LB method is the discrete Boltzmann equation formulated for a two-dimensional geometry as

$$\frac{\partial f_i}{\partial t} + \mathbf{e}_i \cdot \nabla f_i = J_i + \mathbf{e}_i \cdot F_i, \qquad i = 1, 2, \ldots, N, \tag{3.1}$$

where f_i is the particle distribution function which denotes the number of particles at the lattice node $\mathbf{x}=(x,y)^T$ and time t moving in direction i with velocity $\mathbf{e}_i$ along the lattice $\Delta x = \Delta y = \mathbf{e}_i \Delta t$ connecting the nearest neighbors and N is the total number of directions in a lattice. In (3.1), J_i represents the collision term and F_i includes the effect of external forces. Using the single time relaxation of the Bhatanagar-Gross-Krook (BGK) approach [8], the discrete collision term is given by

$$J_i = -\frac{1}{\tau} \left(f_i - f_i^{eq} \right), \tag{3.2}$$

where τ is the relaxation time and f_i^{eq} is the equilibrium distribution function.

In the current work we consider the D2Q9 square lattice model [25], as depicted in Fig. 1. The nine velocities $\mathbf{e}_i$ in the D2Q9 lattice are defined by

$$\mathbf{e}_i = \begin{cases} (0,0)^T, & i = 0, \\ \left(\cos\left((i-1)\frac{\pi}{4}\right), \sin\left((i-1)\frac{\pi}{2}\right) \right)^T c, & i = 1,2,3,4, \\ \left(\cos\left((i-5)\frac{\pi}{2} + \frac{\pi}{4}\right), \sin\left((i-5)\frac{\pi}{2} + \frac{\pi}{4}\right) \right)^T \sqrt{2}c, & i = 5,6,7,8, \end{cases} \tag{3.3}$$

where $c=\Delta x/\Delta t=\Delta y/\Delta t$. Here, Δt is chosen such that the particles travel one lattice spacing during the time step. The corresponding weights w_i to the above velocities are

$$w_i = \begin{cases} 4/9, & i = 0, \\ 1/9, & i = 1,2,3,4, \\ 1/36, & i = 5,6,7,8. \end{cases} \tag{3.4}$$

The selection of the relaxation time τ and the equilibrium distribution function f_i^{eq} in (3.2) depend on the macroscopic equations under study. Next, we describe the formulation of these parameters for the shallow water equations (2.9b) and the depth-averaged convection-diffusion equation (2.10).
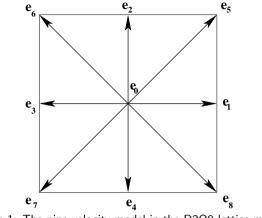
Figure 1: The nine-velocity model in the D2Q9 lattice model.

3.1   The Lattice Boltzmann method for free-surface flow

For the shallow water equations (2.9b), the equilibrium distribution function f_i^{eq} depends on the water depth h and the velocity field $\mathbf{U}=(U,V)^T$ which are recovered by

$$h(\mathbf{x},t) = \sum_{i=0}^{N-1} f_i, \qquad h(\mathbf{x},t)\mathbf{U}(\mathbf{x},t) = \sum_{i=0}^{N-1} \mathbf{e}_i f_i, \tag{3.5}$$

where $\mathbf{U}=(U,V)$ denotes the velocity field in (2.9b). For the D2Q9 lattice, the equilibrium function f_i^{eq} in (3.2) is defined as [12,27]

$$f_i^{eq} = \begin{cases} h - w_0 h\left(\dfrac{15}{2}gh - \dfrac{3}{2}\mathbf{U}^2\right), & i=0, \\ w_i h\left(\dfrac{3}{2}gh + 3\mathbf{e}_i\cdot\mathbf{U} + \dfrac{9}{2}(\mathbf{e}_i\cdot\mathbf{U})^2 - \dfrac{3}{2}\mathbf{U}^2\right), & i=1,\dots,8, \end{cases} \tag{3.6}$$

with the weight factors w_i in (3.4). It is easy to verify that the local equilibrium function satisfies the following conditions

$$\sum_{i=0}^{8} f_i^{eq} = h, \qquad \sum_{i=0}^{8} \mathbf{e}_i f_i^{eq} = h\mathbf{U}, \qquad \sum_{i=0}^{8} \mathbf{e}_i \otimes \mathbf{e}_i f_i^{eq} = \frac{1}{2}gh^2\mathbf{I} + h\mathbf{U}\otimes\mathbf{U}, \tag{3.7}$$

where $\mathbf{I}$ denotes the 2×2 identity matrix. The central idea in the LB method lies essentially in the recovery of the macroscopic flow behaviour from the microscopic flow picture of the particle movement.

   After discretization, equation (3.2) can be written as

$$f_i(\mathbf{x} + \mathbf{e}_i\Delta t, t + \Delta t) = f_i(\mathbf{x},t) - \frac{\Delta t}{\tau_f}\left[f_i - f_i^{eq}\right] + 3\Delta t w_i \mathbf{e}_i \cdot \mathbf{F}, \tag{3.8}$$

where **F** represents the force term in the shallow water equations (2.9b)

$$\mathbf{F} = \begin{pmatrix} -g'h\dfrac{\partial B}{\partial x} - g\alpha h\dfrac{\partial (h\Theta)}{\partial x} + \dfrac{\mathcal{T}_x^\omega}{\rho} - \dfrac{\mathcal{T}_x^b}{\rho} - \Omega hV \\[4mm] -g'h\dfrac{\partial B}{\partial y} - g\alpha h\dfrac{\partial (h\Theta)}{\partial y}\dfrac{\mathcal{T}_y^\omega}{\rho} - \dfrac{\mathcal{T}_y^b}{\rho} + \Omega hU \end{pmatrix}. \tag{3.9}$$

By applying a Taylor expansion and the Chapman-Enskog procedure to equation (3.8), it can be shown that the solution of the discrete lattice Boltzmann equation (3.8) with the equilibrium function (3.6) results in the solution of the shallow water equations (2.9b). The external force terms such as wind stress, Coriolis force, and bottom friction are easily included in the model by introducing them into the force term **F**. For details on this multi-scale expansion, we refer to [12, 27, 42].

To complete the formulation of LB method for equations (2.9b), the relaxation time τ_f has to be defined. In our LB implementation, the relaxation time is determined by the physical viscosity in (2.9b) and the time step through the formula

$$\tau_f = \frac{3\nu_H}{c^2} + \frac{\Delta t}{2}. \tag{3.10}$$

In the lattice Boltzmann method, equation (3.8) is solved in two steps: collision and streaming. In the collision step, the equations for each direction are relaxed toward equilibrium distributions. Then, at the streaming step, the distributions move to the neighboring nodes.

3.2 The lattice Boltzmann method for free-surface temperature

The LBM for transport equation (2.10) is derived using a similar approach as the one used for the shallow water equations (2.9b). Hence, starting from equation (3.2) and using the D2Q9 lattice form Fig. 1, a lattice Boltzmann discretization of the transport equation is

$$g_i(\mathbf{x} + \mathbf{e}_i\Delta t, t + \Delta t) - g_i(\mathbf{x}, t) = -\frac{\Delta t}{\tau_g}\left[g_i - g_i^{eq}\right] + \Delta t\mathcal{Q}_i, \tag{3.11}$$

where g_i is the distribution function, τ_g is the relaxation time and $\mathcal{Q}_i$ is the source term associated with the convection-diffusion equation (2.10). In (3.11), g_i^{eq} is an equilibrium distribution function satisfying the following conditions

$$\sum_{i=0}^{8} g_i = \sum_{i=0}^{8} g_i^{eq} = h\Theta, \qquad \sum_{i=0}^{8} \mathbf{e}_i g_i = \sum_{i=0}^{8} \mathbf{e}_i g_i^{eq} = \mathbf{U}h\Theta. \tag{3.12}$$

To process equation (3.11), a relaxation time and equilibrium function are required. For the convection-diffusion equation, the equilibrium function is given by

$$g_i^{eq} = w_i h\Theta\left[1 + 3\mathbf{e}_i \cdot \mathbf{U}\right], \tag{3.13}$$

where the lattice weights w_i are defined in (3.4). For this selection, the source term in (3.11) is set to

$$\mathcal{Q}_i = w_i h Q. \tag{3.14}$$

It should be noted that the convection-diffusion equation (2.10) can be obtained from equation (3.11) using the Chapman-Enskog expansion. Details on these derivations were given in [5]. It should be stressed that a similar approach was applied in [11] for reaction-diffusion equations.

As in the LB method for shallow water equations, the relaxation time is defined by the thermal diffusion coefficient in (2.10) and the time step as

$$\tau_g = \frac{3\lambda}{c^2} + \frac{\Delta t}{2}. \tag{3.15}$$

Notice that conditions (3.10) and (3.15) give the relation between the lattice diffusion and the time step to be used in the LB simulations.

3.3 Boundary conditions

It well established that implementation of boundary conditions in the LB method has a crucial impact on the accuracy and stability of the method, see [14, 46] for more discussions. When no-slip boundary conditions for the flow velocities are imposed at walls, the bounce-back rule is usually used in the LB algorithm. At a boundary point x_b, populations f_i of links $\mathbf{e}_i$ which intersect the boundary and point out of the fluid domain are simply reflected (bounce-back) since they cannot participate in the normal propagation step

$$f_{i^*}(\mathbf{x}_b, t + \Delta t) = f_i(\mathbf{x}_b, t), \qquad \text{index } i^* \text{ s.t. } \mathbf{e}_{i^*} = -\mathbf{e}_i.$$

For the numerical examples considered in the present study, flow boundary conditions for the height, H, and/or the velocities, (U, V), are needed at the inlet and the outlet of computational domains. When the height H_l is prescribed at the left boundary, the three distributions f_1, f_5 and f_8 are unknown. We use the techniques described in [43,46] for flat interfaces to implement these boundary conditions in the framework of LB method. Assuming that $V = 0$, the velocity in x-direction can be recovered from the relation

$$H_l U = H_l - \Big(f_0 + f_2 + f_4 + 2(f_3 + f_6 + f_7) \Big),$$

and we define the unknown distributions as

$$f_1 = f_3 + \frac{2}{3} H_l U, \tag{3.16a}$$

$$f_5 = f_7 - \frac{1}{2}(f_2 - f_4) + \frac{1}{6} H_l U, \tag{3.16b}$$

$$f_8 = f_6 + \frac{1}{2}(f_2 - f_4) + \frac{1}{6} H_l U. \tag{3.16c}$$

Neumann boundary conditions are implemented by imposing the equilibrium distribution corresponding to the prescribed height, H_l, and the velocity of the nearest neighbor in direction of the normal, (U_n, V_n)

$$f_i = f_i^{eq}(H_l, U_n, V_n), \qquad i = 0, 1 \ldots, 8.$$

Dirichlet boundary conditions for the prescribed temperature Θ_0 can be imposed by the equilibrium for the unknown populations

$$g_i = g_i^{eq}(\Theta_0, U, V), \qquad i = 0, 1 \ldots, 8.$$

Neumann boundary conditions are also frequently used in convection-diffusion problems. They are implemented in the LB framework in a similar way by prescribing the concentration of the neighbour node Θ_n at the boundary

$$g_i = g_i^{eq}(\Theta_n, U, V), \qquad i = 0, 1 \ldots, 8.$$

For the simulation of sea-temperature dispersion in the Strait of Gibraltar, we have flow boundary conditions for the water height and a Neumann boundary condition for the velocity. These boundary conditions are implemented by imposing the equilibrium distribution corresponding to the prescribed height, H_0, and the velocity of the nearest neighbor in the direction of the normal (U_n, V_n)

$$f_i = f_i^{eq}(H_0, U_n, V_n), \qquad i = 0, 1 \ldots, 8.$$

Moreover, for the convection-diffusion LB equation in the test example of the Strait of Gibraltar, boundary conditions at the coastlines and the open sea boundaries are required. We impose fixed temperature (Dirichlet) boundary conditions at the coastlines and Neumann boundary conditions for the temperature at the western and eastern ends of the Strait of Gibraltar.

Other types of boundary conditions can also be incorporated. For further details on the implementation of general boundary conditions for lattice Boltzmann shallow water models we refer the reader to [5, 14, 34, 46]. General details on the implementation of an LB method for irregular domains can also be found in [20, 36] among others.

4   Numerical examples

In this section the accuracy and performance of the LB scheme is tested. Three test examples are used: a tidal flow problem, an advection-diffusion of a Gaussian pulse in a uniform rotating flow field, and simulation of free-surface temperature in the Strait of Gibraltar. The former first tests have analytical solutions that can be used to quantify error in the LB method while the latter is used to qualify LB results for more complicated free-surface flows. In all the examples, the gravitation constant g is taken as 9.81 m/s^2, the time step is chosen according to the latice sizes as well as with stability conditions given in (3.10) and (3.15).

4.1 Tidal wave problem

This example was used in [7], in which an asymptotic analytical solution was obtained. Here, a channel with length $L = 14$ *Km* is considered with a bed elevation defined by

$$Z(x) = 10 + \frac{40x}{L} + 10\sin\left(\pi(\frac{4x}{L} - \frac{1}{2})\right).$$

The bottom frictions, wind stresses and Coriolis effect were neglected in this test. If we take the initial and boundary conditions as

$$H(x,0) = 60.5 - Z(x), \qquad U(x,0) = 0,$$
$$H(0,t) = 64.5 - 4\sin\left(\pi(\frac{4t}{86400} + \frac{1}{2})\right), \qquad U(L,t) = 0,$$

an analytical solution, based on the asymptotic analysis, can be given by [7]

$$\tilde{H}(x,t) = 64.5 - Z(x) - 4\sin\left(\pi(\frac{4t}{86400} + \frac{1}{2})\right),$$
$$\tilde{U}(x,t) = \frac{(x-L)\,\pi}{5400h(x,t)}\cos\left(\pi(\frac{4t}{86400} + \frac{1}{2})\right).$$

This asymptotic analytical solution is used to quantify the results obtained by the LB method. We compute the L^∞-, L^1- and L^2-error norms as

$$L^1 = \sum_{i=1}^{N}|E_i^n|\,\Delta x, \qquad L^2 = \left(\sum_{i=1}^{N}|E_i^n|^2\,\Delta x\right)^{frac12}, \qquad L^\infty = \max_{1\leq i\leq N}|E_i^n|, \qquad (4.1)$$

where $E_i^n = U_i^n - \tilde{U}(x_i, t_n)$ is the error between the numerical solution, U_i^n, and the analytical solution, $\tilde{U}(x_i, t_n)$, at time t_n and lattice point x_i. We used $\tau_H = 0.6$, $c = 200$ m/s
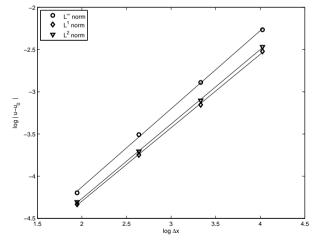

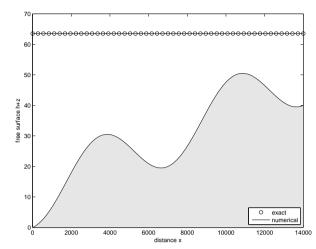Figure 2: Error plots for the tidal wave flow at time $t = 9117.5s$.

Figure 3: Numerical and analytical free-surface for the tidal wave flow at time t=9117.5s.

and the results are displayed at time t=9117.5s. For this test example the ratio U/c= 0.0009. Note that we used a two-dimensional code to reproduce numerical solutions for the one-dimensional problem. Therefore, boundary conditions in the y-direction have to be supplied for the two-dimensional code. For this test example, the dimension in y-direction is fixed to 50 lattice points. Periodic boundary conditions are assumed on the upper and lower walls.

In Fig. 2, we display the error norms for the velocity solution using four uniform lattices with sizes Δx=Δy=56 m, 28 m, 14 m and 7 m at the considered time. A logarithmic scale is used on the x- and y-axis. It is clear that decreasing the lattice size results in a decrease of all error norms. Similar results, not reported here, are obtained focusing the attention on the water depth. As expected the LB method shows a first-order accuracy for this nonlinear example.

Fig. 3 presents the numerical and analytical solutions for the water free-surface at the simulation time t=9117.5 s using a lattice size of Δx=Δy=7 m. It is clear the good agreement between the asymptotic analytical solution and the numerical results obtained by the LB method using the coarse lattice. The LB method performs well for this unsteady shallow water problem and produces accurate solutions without requiring special treatment of the source terms or complicated upwind discretization of the gradient fluxes as in [7] among others.

4.2 Advection-dispersion problem

In this example we will test the accuracy of LB method for an advection-dispersion equation with a prescribed velocity field and known analytical solution. Hence, we solve the equation (2.10) with constant water depth

$$\frac{\partial \Theta}{\partial t} + \frac{\partial}{\partial x}(U\Theta) + \frac{\partial}{\partial y}(V\Theta) - \lambda \Delta \Theta = 0. \tag{4.2}$$

We consider the test problem of the advection-dispersion of a Gaussian pulse in a uniform rotating flow field proposed in [31]. Thus, the computational domain is a 3200 *km* long square equipped with the initial condition

$$\Theta(x,y,0) = 100 \exp\left(-\frac{(x-x_0)^2 + (y-y_0)^2}{2\sigma^2}\right), \tag{4.3}$$

where $(x_0, y_0) = (-800 \, km, 0)$ is the centre of the initial Gaussian and $\sigma = 2 \times 10^4 \, km^2$. As in [31] we take $U = -\omega y$ and $V = \omega x$, with $\omega = 10^{-5}/s$ being the angular velocity. It is easy to verify that the problem (4.2)-(4.3) has an exact solution given by

$$\tilde{\Theta}(x,y,t) = \frac{100}{1 + \frac{2\lambda t}{\sigma^2}} \exp\left(-\frac{\bar{x}^2 + \bar{y}^2}{2(\sigma^2 + 2\lambda t)}\right), \tag{4.4}$$

with

$$\bar{x} = x - x_0 \cos \omega t + y_0 \sin \omega t, \quad \bar{y} = y - x_0 \sin \omega t - y_0 \cos \omega t.$$

Two diffusivity coefficients namely, $\lambda = 10^4 \, m^2/s$ and $2 \times 10^4 \, m^2/s$ are considered. To check the accuracy of the LB method for this test problem, a simulation is carried out until a full rotation of the Gaussian is completed using different lattice sizes, L^1, L^2 and L^∞ norms of the errors are computed using (4.1). We used homogeneous Neumann boundary conditions on all domain boundaries, and we set $\hat{D} = 0.01$.

In Table 1, the accuracy analysis results, obtained considering four different lattice steps, are summarized. For the selected diffusivity coefficients, a decay behaviour is observed for each increase of the number of lattice points. A slower decay is seen for computations with $\lambda = 2 \times 10^3 \, m^2/s$ than those computed with $\lambda = 10^3 \, m^2/s$. This fact can be attributed to the large physical diffusion in the advection-dispersion problem such that the Gaussian spreads strongly and the solution is significantly different from zero at the boundaries and outside of the domain. It is evident, however, that our LB method converges to the correct solution also for this advection-dispersion problem.

Surface plots of the solution at times $t = T/4$, $T/2$, $3T/4$ and T are presented in Fig. 4. Those corresponding to contour plots are displayed in Fig. 5. Here, we used

$$\lambda = 10^3 \, m^2/s, \quad \Delta x = \Delta y = 100 \, Km, \quad T = 628318 \, s,$$

which corresponds to the time necessary for a complete rotation. In the figures, we can clearly see that there are no spurious numerical oscillations in vicinity of the Gaussian pulse, verifying the of the LB method.

Table 1: L^1, L^2 and L^∞ errors for the advection-dispersion problem after a complete rotation.

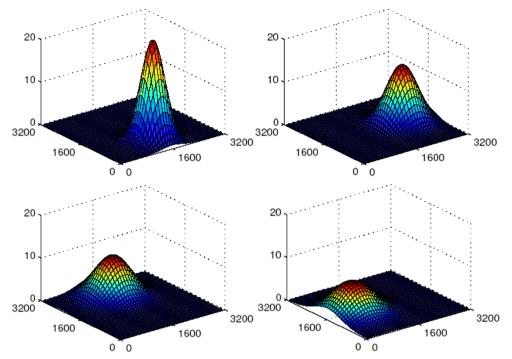| N	$\lambda = 10^3 \, m^2/s$			$\lambda = 2 \times 10^3 \, m^2/s$		
	L^∞-error	L^1-error	L^2-error	L^∞-error	L^1-error	L^2-error
40	3.733E-02	2.338E-02	2.416E-02	2.435E-03	2.293E-02	1.856E-02
80	9.650E-03	5.811E-03	6.093E-03	2.435E-03	7.170E-03	5.944E-03
160	2.935E-03	1.456E-03	1.527E-03	4.940E-03	3.218E-03	3.658E-03
320	6.098E-04	3.679E-04	3.821E-04	3.907E-03	2.067E-03	2.277E-03

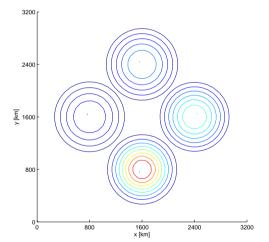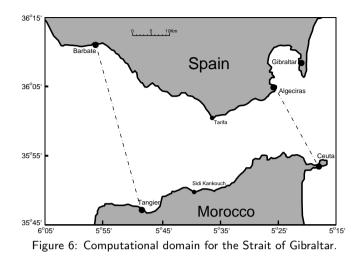Figure 4: Surface plots for the advection-dispersion problem at four different times.

Figure 5: Contour plots for the advection-dispersion problem at four different times.

4.3 Free-surface temperature in the Strait of Gibraltar

The purpose of this test problem is to examine the performance of our LB model for simulating sea-surface temperature in the Strait of Gibraltar. The basic circulation in the Strait of Gibraltar consists in an upper layer of cold, fresh surface Atlantic water and an opposite deep current of warmer, salty Mediterranean outflowing water, compare [3,15]. The sea-surface temperatures in the Strait of Gibraltar are maxima in

Figure 6: Computational domain for the Strait of Gibraltar.

summer (August-September) with average values of 23-24°C and minima in winter (January-February) with averages of 11-12°C. The north Atlantic water is about 5-6°C colder than the Mediterranean water, elaborate details are available in [21,24].

Fig. 6 shows the computational domain used in our simulations along with major locations in the Strait of Gibraltar. The domain is about 60 *Km* long between its west Barbate-Tangier section and its east Gibraltar-Ceuta section. Its width varies from a minimum of about 14 *Km* at Tarifa-Punta Cires section and a maximum of 44 *Km* at Barbate-Tangier section. Here, the simulation domain is restricted by the Tangier-Barbate axis from the Atlantic ocean and the Ceuta-Algeciras axis from the Mediterranean. This domain is taken in the simulation mainly because measured data is usually provided by stations located on the above mentioned cities. Therefore, we have adapted the same domain for our simulations. In addition, vast water areas of the Strait of Gibraltar is shallow with less than 1 *Km* maximum depth. In the present study we consider a reconstructed bathymetry from [15] as depicted in Fig. 7.

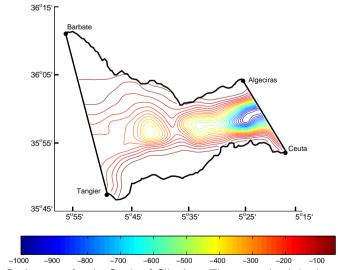In all our simulations, the Chezy friction coefficient $C_z = h^{1/6}/\eta$ with $n_b = 0.012 s/m^{1/3}$

Figure 7: Bathymetry for the Strait of Gibraltar. The water depth is given in meters.

is the Manning constant, the coefficient of wind friction $C_\omega = 10^{-5}$, the Coriolis parameter $\Omega = 8.55 \times 10^{-5}$ $1/s$, and the horizontal eddy viscosity of $\nu_H = 100$ m^2/s, see for example [15,33]. A mesh with lattice size $\Delta x = \Delta y = 250$ m is used for all the results presented in this section. This mesh structure has been selected after a grid independence study assessed by comparing numerical results obtained using different meshes, compare [34] for more details. Depending on the wind conditions, three situations are simulated namely:

1. Calm situation corresponding to $(\omega_x = 0 \ m/s, \omega_y = 0 \ m/s)$;
2. Wind blowing from the east corresponding to $(\omega_x = -1 \ m/s, \omega_y = 0 \ m/s)$;
3. Wind blowing from the west corresponding to $(\omega_x = 1 \ m/s, \omega_y = 0 \ m/s)$.

A no-slip boundary condition for velocity variables has been applied at the coastal boundaries. At the open boundaries, Neumann boundary conditions are imposed for the velocity, and the water elevation is prescribed as a periodic function of time using the main semidiurnal and diurnal tides. The tidal constants at the open boundary lattice nodes were calculated by interpolation from those measured at the coastal stations Tangier and Barbate on the western end and the coastal stations Ceuta and Algeciras on the eastern end of the Strait. We considered the main semidiurnal M_2, S_2 and N_2 tidal waves, and the diurnal K_1 tidal wave in the Strait of Gibraltar. Thus,

$$
\begin{aligned}
H = H_0 &+ A_{M_2} \cos\left(\omega_{M_2} t + \varphi_{M_2}\right) + A_{S_2} \cos\left(\omega_{S_2} t + \varphi_{S_2}\right) \\
&+ A_{N_2} \cos\left(\omega_{N_2} t + \varphi_{N_2}\right) + A_{K_1} \cos\left(\omega_{K_1} t + \varphi_{K_1}\right),
\end{aligned} \tag{4.5}
$$

where A_k is the wave amplitude, ω_k the angular frequency and φ_k the tide phase for the considered tide k, with $k = M_2$, S_2, N_2 or K_1. The measured data for these parameters are provided for the cities defining the computational domain and are given in [5, 15]. In (4.5), H_0 is the averaged water elevation set to $3m$ in our simulations. Initially, the simulated flow has been at warm rest, i.e.,

$$
U = V = 0, \qquad H = H_0 \qquad \text{and} \qquad \Theta = \Theta_h, \tag{4.6}
$$

where $\Theta_h = 23°C$ is the Mediterranean temperature and the western temperature boundary of the Strait is fixed to the Ocean temperature $\Theta_c = 17°C$. Note that, in order to ensure that the initial conditions of the water flow and sea-surface temperature are consistent we proceed as follows. The shallow water equations (2.9b) are solved without temperature dispersion for two weeks of real time to obtain a well-developed flow. The obtained results are taken as the real initial conditions and the sea-surface temperature is included at this stage of the simulation. At the end of the simulation time the velocity fields and temperature contours are displayed after 12, 18 and 24 hours from the inclusion of sea-surface temperature.

In Fig. 8, we present numerical results obtained using calm wind conditions. Those obtained for the wind blowing from the east and the wind blowing from the west are displayed in Figs. 9 and 10, respectively. In these figures, we show the velocity field and 10 equi-distributed contours between Θ_c and Θ_h of the temperature at the instants
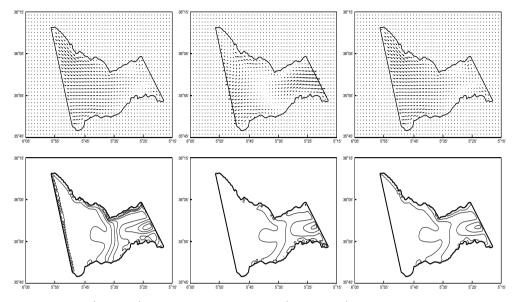
Figure 8: Flow field (first row) and temperature contours (second row) for calm situation at three different times. From left to right t=12, 18 and 24 hours.

t=12, 18 and 24 hours. It is clear that using the conditions for the tidal waves and the considered wind situations, the flow exhibits a recirculating zone with different order of magnitudes near the Caraminal Sill (*i.e.* the interface separating the water bodies betwen the Mediterranean sea and the Atlantic Ocean). At the beginning of simulation time, the water flow enters the Strait from the eastern boundary and flows towards the eastern exit of the Strait. At later time, due to tidal waves, the water flow changes the direction pointing towards the Atlantic Ocean. A recirculating flow region is also
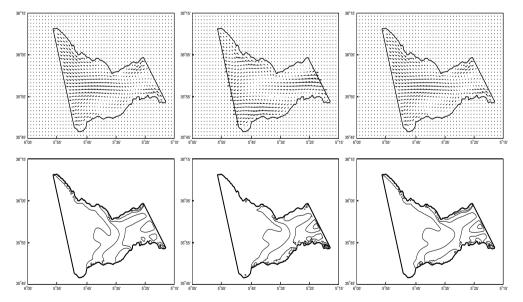

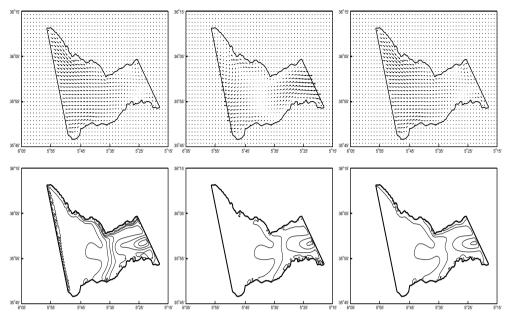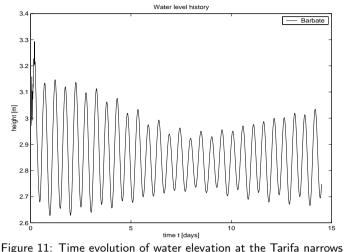Figure 9: The same as in Fig. 8 but for a wind blowing from the east.

Figure 10: The same as in Fig. 8 but for a wind blowing from the west.

detected on the top eastern exits of the strait near Algeciras. Similar flow behaviours have been also reported in [3, 15, 34].

The effects of wind conditions are observed in the temperature distributions presented in Figs. 8, 9 and 10. A boundary layer of high sea-surface temperatures has been detected on the Spanish coastal lines. For the considered tides and wind conditions, the buoyancy force has been seen to play a weak role for driven the sea-surface tamperature in the Strait of Gibraltar which results in thiner mixing layers. In Figure 11 we display the time evolution of the water free-surface elevation at the Tarifa narrows for a time period of two weeks. As expected, the time series show two tidal periods with different amplitude and frequencies. They are in good agreement with those previously computed in [9, 33]. Similar results not presented here, have been obtained at other locations in the Strait of Gibraltar.

Note that the proposed lattice Boltzmann shallow water model performs well for this test problem since it does not diffuse the moving fronts and no spurious oscillations have been observed near steep gradients of the flow field in the computational domain. It can be clearly seen that the complicated flow structures on the Caraminal Sill and near Tarifa narrows and Tangier basin are being captured by the LB method. In addition, the presented results clearly indicate that the method is suited for prediction of sea-surface temperature dispersion in the Strait of Gibraltar. It should be stressed that ideally, results from the temperature dispersion model should be compared with observations of real sea-surface temperatures in the Strait of Gibraltar. However, there are no available data until now to carry out this work. Thus, we could only simulate some hypothetical simulations simply to show that LB results are logical and consistent.

Figure 11: Time evolution of water elevation at the Tarifa narrows.

5   Conclusions

In this paper, an accurate and stable numerical algorithm is implemented, using the lattice Boltzmann method, for the solution of free-surface temperature dispersion in the shallow water flows. The model has been derived from a depth-averaged incompressible Navier-Stokes equations including bed frictions, eddy viscosity, wind shear stresses and Coriolis forces. The coupling between the water flow and the free-surface temperature is modelled using the Boussinesq approximation. A depth-averaged advection-diffusion equation has been used to describe the dispersion of temperature on the water free-surface.

The numerical method is based on single relaxation BGK models, and it is characterized by two distribution functions in the lattice Boltzmann method to recover the flow and temperature variables using the same lattice structure. The method is simple, accurate, easy to implement, and can be used to solve both steady and unsteady depth-averaged problems. The method also provides a straightforward treatment of source terms without relying on complicated discretization techniques. More precisely, the method avoids (i) Riemann solvers, (ii) well- balanced discretization of gradient terms and source terms in the shallow water equations, (iii) iterative solvers required for convection-diffusion problems, and (iv) special treatment of irregular domain and complex bathymetry.

To demonstrate the performance and the capability of the algorithm, the method has been applied to solve classical test problems, both on shallow water and advection-diffusion equations. Then, the algorithm is applied to solve the sea-surface temperature dispersion in the Strait of Gibraltar. This last example represents a practical example for the lattice Boltzmann shallow water flow for two major reasons. Firstly, the computational domain in the Strait of Gibraltar is a large-scale domain including high gradients of the bathymetry and well-defined shelf regions. Secondly, the

Strait contains complex fully two-dimensional tidal flow structures, eddy viscosity, Coriolis forces and wind shear stresses, which present a challenge for most numerical methods used for the shallow water modelling. The presented results demonstrate the accuracy of the lattice Boltzmann method and its capability to simulate tidal flows and sea-surface temperature transport in the hydrodynamic regimes considered.

Acknowledgments

References

[1] F. ALCRUDO AND F. BENKHALDOUN, *Exact solutions to the Riemann problem of the shallow water equations with a bottom step*, Comput. Fluids., 30 (2001), pp. 643-671.

[2] F. ALCRUDO AND P. GARCIA-NAVARRO, *A high resolution Godunov-type scheme in finite volumes for the 2D shallow water equation*, Int. J. Numer. Methods in Fluids., 16 (1993), pp. 489-505.

[3] J.I. ALMAZÁN, H. BRYDEN, T. KINDER AND G. PARRILLA, Seminario Sobre la Oceanografía Física del Estrecho de Gibraltar, SECEG, Madrid, (1988).

[4] E. AUDUSSE, F. BOUCHUT, M.O. BRISTEAU, R. KLEIN AND B. PERTHAME, *A fast and stable well-balanced scheme with hydrostatic reconstruction for shallow water flows*, SIAM J. Sci. Comp., 25 (2004), pp. 2050–2065.

[5] M.K. BANDA, M. SEAÏD AND G. THÖMMES, *Lattice Boltzmann simulation of dispersion in two-dimensional tidal flows*, International Journal for Numerical Methods in Engineering, 77 (2009), pp. 878–900.

[6] A. BARTZOKAS, *Estimation of the eddy thermal diffusivity coefficient in water*, J. Meteorology and Atmospheric Physics, 33 (1985), pp. 401–405.

[7] A. BERMÚDEZ AND M.E. VÁZQUEZ, *Upwind methods for hyperbolic conservation laws with source terms*, Computers & Fluids, 23 (1994), pp. 1049–1071.

[8] P. BHATNAGAR, E. GROSS AND M. KROOK, *A model for collision process in gases*, Phys. Rev. Lett., 94 (1954), pp. 511–525.

[9] M.J. CASTRO, J.A. GARCÍA-RODRÍGUEZ, J.M. GONZÁLEZ-VIDA, J. MACÍAS, C. PARÉS AND M.E. VÁZQUEZ-CENDÓN, *Numerical simulation of two-layer shallow water flows through channels with irregular geometry*, J. Comp. Physics., 195 (2004), pp. 202–235.

[10] DUDLEY B. CHELTON, STEVEN K. ESBENSEN, MICHAEL G. SCHLAX, NICOLAI THUM, MICHAEL H. FREILICH, FRANK J. WENTZ, CHELLE L. GENTEMANN, MICHAEL J. MCPHADEN AND PAUL S. SCHOPF, *Observations of coupling between surface wind stress and sea surface temperature in the Eastern Tropical Pacific*, Journal of Climate, 14 (2001), pp. 1479–1498.

[11] S.P. DAWSON, S. CHEN AND G.D. DOOLEN, *Lattice Boltzmann computations for reaction-diffusion equations*, J. Chem. Phys., 98 (1993), pp. 1514–1523.

[12] P.J. DELLAR, *Non-hydrodynamic modes and a priori construction of shallow water lattice Boltzmann equations*, Phys. Rev. E (Stat. Nonlin. Soft Matter Phys., 65 (2002), 036309 (12 Pages).

[13] S. FENG, Y. ZHAO, M. TSUTAHARA AND Z. JI, *Lattice Boltzmann model in rotational flow field*, Chinese J. of Geophys., 45 (2002), pp. 170–175.

[14] M.A. GALLIVAN, D.R. NOBLE, J.G. GEORGIADS AND R.O. BUCKIUS, *An evaluation of the bounce-back boundary condition for lattice Boltzmann simulations*, Int. J. Num. Meth. Fluids., 25 (1997), pp. 249–263.

[15] M. GONZÁLEZ AND A. SÁNCHEZ-ARCILLA, *Un Modelo Numérico en Elementos Finitos para la Corriente Inducida por la Marea. Aplicaciones al Estrecho de Gibraltar*, Revista Internacional de Métodos Numéricos para Cálculo y Diseño en Ingeniería., 11 (1995), pp. 383–400.

[16] J.H. LaCASCE AND A. MAHADEVAN, *Estimating sub-surface horizontal and vertical velocities from sea surface temperature*, J. Mar. Res., 64 (2006), pp. 695–721.

[17] J.G. LAFUENTE, J.L. ALMAZÁN, F. CATILLEJO, A. KHRIBECHE AND A. HAKIMI, *Sea level in the strait of Gibraltar: Tides*, Int. Hydrogr. Rev. LXVII., 1 (1990), pp. 111–130.

[18] R.J. LEVEQUE, *Balancing source terms and the flux gradients in high-resolution Godunov methods: the quasi-steady wave-propagation algorithm*, J. Comput. Phys., 146 (1998), pp. 346–365.

[19] A. KURGANOV AND D. LEVY, *Central-upwind schemes for the Saint-Venant system*, Math. Model. Numer. Anal., 36 (2002), pp. 397–425.

[20] R. MEI, L.S. LUO AND W. SHYY, *An accurate curved boundary treatment in the Lattice Boltzmann method*, J. Comput. Phys., 1999; 155 (1999), pp. 307–330.

[21] M. MILLÁN, M.J. ESTRELA AND V. CASELLES, Torrential Precipitations on the Spanish East Coast: The role of the mediterranean sea surface temperature, Atmospheric Research, 36 (1995), pp. 1–16.

[22] T. MING-HEN, *The improved surface gradient method for flows simulation in variable bed topography channel using TVD-MacCormack scheme*, Int. J. Numer. Methods in Fluids., 43 (2003), pp. 71–91.

[23] B. PERTHAME AND C. SIMEONI, *A kinetic scheme for the Saint-Venant system with a source term*, CALCOLO., 38 (2001), pp. 201–231.

[24] B.G. POLYAK, M. FERNÁNDEZ, M.D. KHUTORSKOY, J.I. SOTO, I.A. BASOV, M.C. COMAS, V.YE. KHAIN, B. ALONSO, G.V. AGAPOVA, I.S. MAZUROVA, A. NEGREDO, V.O. TOCHITSKY, J. DE LA LINDE, N.A. BOGDANOV AND E. BANDA, Heat flow in the Alboran Sea, Western Mediterranean. Tectonophysics, 263 (1996), pp. 191–218.

[25] Y.H. QIAN, D. d'HUMIERES AND P. LALLEMAND, *Lattice BGK models for the Navier-Stokes equation*, Europhys. Letters., 17 (1992), pp. 479–484.

[26] P.L. ROE, *Approximate Riemann solvers, parameter vectors and difference schemes*, J. Comp. Phys., 43 (1981), pp. 357-372.

[27] R. SALMON, *The Lattice Boltzmann method as a basis for ocean circulation modeling*, J. Mar. Res., 57 (1999), pp. 503–535.

[28] R. SALMON, *The Lattice Boltzmann solutions of the three-dimensional planetary geostrophic equations*, J. Mar. Res., 57 (1999), pp. 847–884.

[29] J. CLIM, R.M. SAMELSON, E.D. SKYLLINGSTAD, D.B. CHELTON, S.K. ESBENSEN AND L.W. O'NEILL, *Thum N, On the coupling of wind stress and sea surface temperature*, Journal of Climate., 19 (2006), pp. 1557–1566.

[30] M. SEAÏD, *Non-oscillatory relaxation methods for the shallow water equations in one and two space dimensions*, Int. J. Numer. Methods in Fluids., 46 (2004), pp. 457–484.

[31] A. STANIFORTH AND J. CÔTÉ, *Semi-Lagrangian integration schemes for the atmospheric models: A review*, We. Rev., 119 (1991), pp. 2206–2223.

[32] P.K. STANSBY AND J.G. ZHOU, *Shallow water flow solver with non-hydrostatic pressure: 2D vertical plane problems*, Int. J. Numer. Meth. Fluids, 28 (1998), pp. 541–563.

[33] L. TEJEDOR, A. IZQUIERDO, B.A. KAGAN AND D.V. SEIN, *Simulation of the semidiurnal tides in the Strait of Gibraltar*, J. Geophysical Research., 104 (1999), pp. 13541–13557.

[34] G. THÖMMES, M. SEAÏD, M. K. BANDA, *Lattice Boltzmann methods for shallow water flow applications*, Int. J. Num. Meth. Fluids., 55 (2007), pp. 673–692.

[35] E.F. TORO, *Riemann problems and the WAF method for solving two-dimensional shallow water equations*, Phil. Trans. Roy. Soc. Lond. A, 338 (1992), pp. 43–68.

[36] R.G.M. VAN DER SMAN AND M. H. ERNST, *Convection-Diffusion Lattice Boltzmann Scheme for Irregular Lattices*, J. Comput. Phys., 160 (2000), pp. 766–782.

[37] M. VARGAS, T. SARHAN, J. GARCIA LAFUENTE AND N. CANO, *An advection-diffusion model to explain thermal surface anomalies off Cape Trafalgar*, Bol. Inst. Esp. Oceanogr., 15 (1999), pp. 91–99.

[38] M. E. VÁZQUEZ-CENDÓN, *Improved treatment of source terms in upwind schemes for shallow water equations in channels with irregular geometry*, J. Comput. Phys., 148 (1999), pp. 497–526.

[39] S. VUKOVIC AND L. SOPTA, *ENO and WENO schemes with the exact conservation property for one-dimensional shallow-water equations*, J. Comput. Phys., 179 (2002), pp. 593–621.

[40] Y. XING AND C. SHU, *High order well-balanced finite volume WENO schemes and discontinuous Galerkin methods for a class of hyperbolic systems with source terms*, J. Comp. Physics., 214 (2006), pp. 567–598.

[41] K. XU, *Well-balanced gas-kinteic scheme for the shallow water equations with source terms*, J. Comp. Phys., 178 (2002), pp. 533–562.

[42] L. ZHONG, S. FENG AND S. GAO, *Wind-driven ocean circulation in shallow water Lattice Boltzmann Model*, Adv. in Atmospheric Sci., 22 (2005), pp. 349–358.

[43] J.G. ZHOU, *A lattice Boltzmann model for the shallow water equations*, Comput. Method Appl. M., 191 (2002), pp. 3527–3539.

[44] J.G. ZHOU, D.M. CAUSON, C.G. MINGHAM AND D.M. INGRAM, *The surface gradient method for the treatment of source terms in the shallow water equations*, J. Comp. Phys., 20 (2001), pp. 1–25.

[45] J.G. ZHOU, *Velocity-depth coupling in shallow water flows.*, J. Hydr. Engrg., ASCE, 10 (1995), pp. 717–724.

[46] Q. ZOU AND X. HE, *On pressure and velocity boundary condition for the lattice Boltzmann BGK model*, Phys. Fluids., 9 (6) (2002), pp. 1591–1598.